This is a preprint, the final version is subject to change, of the American Mineralogist (MSA)
Cite as Authors (Year) Title. American Mineralogist, in press.
(DOI will not work until issue is live.) DOI: http://dx.doi.org/10.2138/am-2015-5045

REVISION 1

An insight at the inverse transformation of realgar altered by light

Giovanni Pratesi[1,2] and Matteo Zoppi[1*]

[1]Museo di Storia Naturale - Sezione Mineralogia e Litologia, Università di Firenze, via La Pira 4, I-50121 Firenze, Italy.

[2]Dipartimento di Scienze della Terra, Università di Firenze, via La Pira 4, I-50121 Firenze, Italy.

* E-mail: matteo.zoppi@unifi.it

ABSTRACT

The light-induced alteration of realgar and β-As_4S_4 is a well known phenomenon but still displays interesting aspects not completely explained. In the transformation from realgar to pararealgar the molecule As_4S_4 undergoes a structural modification, and ever since the initial studies two important issues have been highlighted: the influence of the oxygen and the reversibility of the process. The previous study on the reversibility of the altered β-As_4S_4 points out that this polymorph exhibits a dual behaviour. When the light-induced alteration occurs with the presence of the air, pararealgar and arsenolite, along with amorphous material, are the products, while if the air is not present β-As_4S_4 turns completely into pararealgar. Moreover, when annealing the altered material in the realgar stability fields (220 °C), in the first case pararealgar and amorphous material turn into stoichiometric alacranite, while in the second case the alteration is completely reversible. Similarly, the present study focuses the

attention on the question if realgar, when altered by means of the light and when annealed, might behave as β-As_4S_4 does. These results display that the phenomenon is more complex. The alteration of realgar with the presence of the air yields pararealgar along with arsenolite, a small quantity of uzonite and amorphous material, and when the air is not present pararealgar is the only product. In the first case, when annealing the products of alteration at 220 °C, alacranite, β-As_4S_4, realgar and little amorphous material occur along with arsenolite. In the second case at first β-As_4S_4 crystallizes, then it turns into realgar, but this process yields orpiment and amorphous material as it moves forwards, showing that from the products of alteration of realgar it is not possible to obtain the starting material. Examination of the stoichiometry of the products let to infer that the amorphous material occurring in the two cases has very different content of arsenic and sulphur.

Keywords: realgar, light, heat, pararealgar, alacranite, uzonite, Rietveld.

INTRODUCTION

The main problem related to the conservation of the mineral realgar is the alteration induced by light that causes opacity, a change from the red colour to yellow, and brittleness of the surface layers. Realgar is not only a mineral with a beautiful red colour and interesting properties of light interaction, it has been employed for many centuries as pigment in manuscripts, paintings and stuccoes in the ancient world and the Renaissance (Corbeil and Helwig 1995; Trentelman et al. 1996; Clark and Gibbs 1997, 1998; Burgio et al. 2003, 2006). From a different point of view future promising employments of realgar may arise from the applications in the field of opto-electronic or from the treatment of various forms of cancer yet investigated *in vitro* and *in vivo* (Lu et al. 2002; Zhao et al. 2009; Liu et al. 2014). More than thirty years ago Roberts et al. (1980) identified pararealgar, a new polymorph of As_4S_4, from

two locations in British Columbia, and pointed out that this mineral was the alteration product of realgar. The pararealgar structure was solved by Bonazzi et al. (1995), after Douglass et al. (1992) studied in detail the phenomenon of light-induced alteration of realgar. Before those studies it was accepted as true that realgar altered to orpiment (As_2S_3) and arsenolite (As_2O_3). Actually the former is related to realgar by paragenetic association and the latter is the product of light-induced alteration, whenever oxygen is present, along with pararealgar. Realgar, α-As_4S_4 ($P2_1/n$), and the polymorph of high temperature, β-As_4S_4 ($C2/c$), display a different packing of the As_4S_4 cage-like molecule (*r*-type) where each As atom is covalently bonded to two S and one As atoms, and each S atom is bonded to two As atoms (Ito et al. 1952; Street and Munir 1970; Mullen and Nowacki 1972). Pararealgar ($P2_1/c$) and the As_4S_4(II) ($P2_1/n$), a synthetically obtained phase (Kutoglu 1976), are made by a different As_4S_4 molecule (*p*-type) with one As atom covalently bonded to one S and two As atoms, two As atoms bonded to one As and two S atoms, and one As atom bonded to three S atoms. Each S atom is bonded to two As atoms. The polymorph β-As_4S_4 (Porter and Sheldrick 1972), is stable over 252 °C (Roland 1972) and durable at room temperature, but undergoes the same phenomenon of alteration when exposed to the light. Douglass et al. (1992) and Bonazzi et al. (1996) pointed out that the action of visible light causes an anisotropic expansion of the unit-cell of both α-As_4S_4 and β-As_4S_4 yielding a metastable product named χ-phase, which is the precursor of pararealgar. Even though not always reported as the product of alteration of realgar, arsenolite occurs starting from both realgar (Ballirano and Maras 2006) and from β-As_4S_4 (Zoppi and Pratesi 2012), and the formation of this oxide is the result of the breaking of As-As and As-S bonds with the presence of oxygen. This phenomenon has been studied, from the structural point of view, for the As_4S_4 polymorphs (Muniz-Miranda et al. 1996; Bonazzi et al. 2006; Bonazzi and Bindi 2008), regarding different species (Bindi et al. 2003; Bonazzi et al. 2003a; Bindi and Bonazzi 2007) and with different conditions of illumination (Kyono 2007;

Naumov et al. 2007). In the accepted model (Kyono et al. 2005), based on the hypothesis of Bindi et al. (2003), the unit-cell expansion of the α and β polymorphs, and the occurrence of the χ-phase, is due to the substitution of As_4S_4 units by As_4S_5 uzonite-type molecules according to the reaction $5As_4S_4 + 3O_2 + h\nu \rightarrow 4As_4S_5 + 2As_2O_3$, and the following release of a sulphur atom to produce the *p*-type molecule according to the reaction $As_4S_5 \rightarrow As_4S_4 + S$. The freed S atom then enters another *r*-type molecule and the mechanism continues in a cyclical pattern. Recent investigations on the light-induced alteration of powdered β-As_4S_4, with and without the presence of the air, led to the observation that the transformation to pararealgar happens in both cases (Zoppi and Pratesi 2012). That suggests that the *r*-type molecule might transform to the *p*-type even without the occurrence of arsenolite. In a closed system, in case the air is not present, the light-induced alteration of β-As_4S_4 yields pure pararealgar, while if the material is in contact with the air, pararealgar, arsenolite and amorphous phase, with assumed formula AsS_2, are produced according to the reaction equation $9As_4S_4 + 3O_2 \rightarrow 7As_4S_4 + 4AsS_2 + 2As_2O_3$. Moreover, if annealing the products of alteration at a temperature of 220 °C – in the stability field of realgar – the inverse transformation from pararealgar to β-As_4S_4 occurs completely when keeping the system isolated from the air. In case the oxygen is present during the light-induced alteration, the inverse transformation of pararealgar plus the amorphous AsS_2 produces stoichiometric alacranite, maintaining the same amount of arsenolite. These results show that the modification from the *r*-type to the *p*-type molecule in the β-As_4S_4 does not depend strictly on the quantity of existing oxygen, and the inverse modification, from the *p*-type to *r*-type molecule, in the altered materials occurs by means of the heat in any case. Different stoichiometry, due to the formation of arsenolite and amorphous AsS_2 keeps the material from transforming into β-As_4S_4 (Zoppi and Pratesi 2012). Furthermore, the observation that in the synthetic adducts $(HgI_2)(As_4S_4)$ and $(HgBr_2)_3(As_4S_4)_2$ the substitution of the *r*-type molecules by the *p*-type ones is the cause of the unit-cell expansion, suggests

that not always the presence of As_4S_5 molecules is required to explain the light-induced transformation of the *r*-type molecules (Bonazzi et al. 2010; Zoppi et al. 2013). In the present study we performed the light-induced alteration of realgar powder, and the following heat-induced inverse transformation, using a combination of unfiltered sunlight and lamp light, so to reproduce more realistically the alteration of the mineral employed as pigment in a work of art. We collected X-ray powder diffraction (XRPD) data from samples of material obtained by the complete alteration of realgar powder, with and without the presence of the air, and after various steps of thermal treatment, similarly to what has been done for the β-As_4S_4 polymorph (Zoppi and Pratesi 2012). The extensive knowledge of this phenomenon might be useful in the field of preservation and restoration of works of art containing realgar as pigment.

EXPERIMENTAL METHODS

XRPD and Rietveld refinements

Some large crystals of realgar, from the locality of Shimen, Hunan Province, China (specimen no. 46768 Museo di Mineralogia dell'Università degli Studi di Firenze), were used as starting material. As reported by Xiong and Liu (1998) the mineral is of high purity with minor traces of Sb as it is assured by the formula $(As_{3.9997}Sb_{0.005})_{\Sigma=4.004}S_4$ based on chemical analyses of samples from this locality. Fragments of the unaltered crystalline realgar were carefully ground in an agate mortar under acetone, keeping the powder in the dark in order to avoid alteration. Half of the realgar powder was sealed in a transparent glass vial containing pure isopropyl alcohol, previously boiled to remove any traces of dissolved oxygen, and the other half was widely spread on a white porcelain mortar as to be always in contact with ambient air. The light-induced alteration of realgar in the two different environments was carried for about 300 hours exposing the materials to unfiltered sunlight as well as lamp light, with the

apparatus described in Zoppi and Pratesi (2012). In order to perform quantitative phase analysis (QPA) with an internal standard, a 10 percent, by weight, of yttrium-III oxide (analytical grade) was added to the powder. The altered materials, placed in a nitrogen purged glove box, were ground and dry, densely packed in 0.5 mm diameter glass capillaries and sealed. Two sets of samples were prepared: capillaries containing realgar powder altered in air, labelled AR, and capillaries containing realgar powder altered under isopropyl alcohol, labelled AL. For all the samples thermal treatments were carried out in a furnace at the constant temperature of 220 °C for a total of 1, 24, 72, 240, 504 and 672 hours, and after each period of time the samples were quenched in air, labelling each sample by adding the suffix of the annealing time (AR24 and AR672 are missing due to the rupture of the capillary caused by the thermal shock). XRPD data collections were carried out, for each sample, using a Panalytical XPert-Pro diffractometer (CuKα radiation at 40 KV, 40 mA) equipped with a focussing mirror, a goniometer (PW3050/60) with theta-theta geometry, a PIXcel solid state detector, and a capillary spinner. On the incident beam a Soller slit (0.04 rad) and a divergence slit (¼ °) were mounted, on the diffracted beam an antiscatter slit (7.50 mm) and a Soller slit (0.04 rad) were mounted. The setting employed for the data collections was the following: 2theta range of 8-120°, step size of 0.01313°, “common counting time” of 197 s, for a total time of 2:03 hours.

Multiphase Rietveld refinements of the structural parameters were performed with the GSAS software (Larson and Von Dreele 2004) with the graphical user interface EXPGUI (Toby 2001). The following items were modelled by refining the corresponding parameters: background contribution (using a Chebyshev polynomial with a variable number of terms), scale factors, lattice parameters, Lorentzian and Gaussian terms of the pseudo-Voigt peak-shape modelling, microstrain line broadening parameters (Stephens 1999), atomic positions and isotropic atomic displacement parameters. The starting structural models, for the phases to be refined, have been taken from literature. Dumping factors were always applied, especially in the first stages of refinements. U_{iso} value for the sulphur atom S2 of alacranite in

the stage AR72 was kept fixed at a value determined averaging U_{iso} of S1, S3, S4, S5 and S6 atoms, since the refined value was unrealistically low. QPA was performed applying the Rietveld-RIR method (Gualtieri 2000) and refining the parameters of the phases occurring in the samples.

Raman micro-spectroscopy and SEM analyses

Raman analyses were carried out employing a confocal Raman microprobe (Horiba Jobin-Yvon LabRam-IR) coupled with an optical microscope and equipped with a HeNe laser source (λ_0 = 632.8 nm), a monochromator with holographic notch filter, a spectrometer with diffraction grating of 1800 gr/mm, and a Peltier cooled CCD detector (1024×256 pixels). On two selected crystals removed from the annealed material contained in the glass capillary at the stage AL672, Raman spectra were collected in the region between 76 and 1120 cm^{-1}, with a slit and hole aperture of 200 μm. A variable integration time of 1 to 5 s, for 4 to 5 accumulation cycles was applied with a laser beam power of 2 mW. The diameter of the laser spot on the sample surface was ~2 μm for the fully focused laser beam at 50× objective magnification. The spectral resolution was 1 cm^{-1} and the instrument was calibrated against the Stokes Raman signal of pure Si at 520 cm^{-1} using a silicon wafer. The second order bands were not analyzed. Instrument control and data acquisition, as well as the processing of Raman spectra, were performed with the software LabSpec 5 (Horiba Jobin-Yvon). SEM analysis have been carried out with a Zeiss EVO MA15 instrument, equipped with an Oxford Inca 250 energy dispersive detector, using the following operating conditions: working distance 9.5 mm, acceleration voltage 20 kV and beam current 0.1 nA.

INTERPRETATION OF DATA AND QPA RESULTS

For the accurate quantification of the As_4S_4 polymorphs, based on the results and assessments reported in Zoppi and Pratesi (2012), the amount of 10%, by weight, of internal standard was added to the

realgar powder so to obtain a good agreement between the lowest error percentage in the QPA and the influence of the peak overlapping effect on the structure refinements. Extrapolating from that case, the estimated uncertainty in the measurement of the crystalline phases using such an amount of internal standard should be not higher than 2.8% (Zoppi and Pratesi 2012). However for the experiments of this study a twofold increase of the common counting time, and a halved step size for all the XRPD data collections, were imposed in order to further reduce the estimated uncertainty of QPA values. XRPD patterns collected before and after the stages of the thermal treatment of the samples AR and AL are shown in the figures 1 and 2, respectively. The data display different results whether the alteration occurs with or without the presence of oxygen. QPA results for the series AR and AL are reported in table 1 and 2, respectively, and in the graphs a) and b) of figure 3, respectively. Estimated uncertainties are not reported for the amorphous fraction since their values are obtained by subtraction, according to the Rietveld-RIR method, and slightly negative values of the weight percent must be considered zero. Moreover a schematic comparison of the results obtained from the present work and the previous studies (Zoppi and Pratesi 2012) are summarized in figure 4.

The alteration of realgar performed with the presence of the air (sample AR) yielded pararealgar, arsenolite, uzonite and amorphous material. The following heat-induced transformation showed that stoichiometric alacranite crystallized at first, while uzonite disappeared, and the amorphous material reduced to few units. Then β-As_4S_4 and realgar occurred, the amount of alacranite decreased, and arsenolite and the amorphous phase remained about constant in every stage of the process. Even if the presence of uzonite in the sample AR could not be observed by Raman micro-spectroscopy, due to the very low quantity dispersed in the bulk material, a clear prove of its occurrence is the presence of its diffraction peaks (figure 5) and the outcome of QPA by means of the full profile fitting with the Rietveld-RIR method. Unfortunately the QPA of the AR504 stage yielded not reliable results as the

weight percent of the amorphous phase is negative (i.e -24.66%). This is due to the presence of crystals of β-As_4S_4 and realgar, more than 100 μm in size and grown on the inner surface of the glass capillary, that cause absorption of the X-ray beam (Cu*K*α) and shielding effects on the scattering power of the Y_2O_3 powder located in the core of the capillary. Moreover the contribution of the orientation effects of the crystals cannot be easily accounted for. This outcome causes an underestimation of the amount of internal standard, thus negative values for the amorphous material, underestimation of alacranite and arsenolite but an overestimation of β-As_4S_4 and realgar. Despite the inaccuracy of the QPA results of the sample AR504, the weight percent values can still be taken as an indication of a trend. In fact the overall QPA values for the process of annealing show that alacranite turns into β-As_4S_4 and realgar, while arsenolite remains approximately constant. Also the amount of the amorphous phase displays little change, but a migration of matter between this and alacranite must occur since a variation of chemical composition, from As_8S_9 to As_4S_4, partially takes place in a closed system.

From the alteration of realgar, carried out under isopropyl alcohol (AL), only pararealgar was obtained and no amorphous material was detected. During the early stages of the heat-induced transformation the expanded form of β-As_4S_4, identified as the χ-phase, occurred, then β-As_4S_4 and realgar crystallized. In the late stages of transformation β-As_4S_4 decreased, while realgar increased in quantity, and eventually a certain amount of orpiment and an increasing values of amorphous material were detected. The occurence of orpiment and realgar, very well developed at the stage AL672, was observed also by SEM secondary electron images, as shown in figure 6 a) and b), respectively. The micro-Raman spectra, collected from the same crystals, prior SEM analysis, are shown in figure 6 c) and d), respectively. EDS analysis of little fragments of irregularly shaped material yielded a chemical composition ranging from pure sulphur to a very variable As:S atomic ratio.

The outcomes of the structural refinements, carried out with the Rietveld method, of the alacranite crystallized in the sample AR72 and the realgar crystallized in the sample AL504 are reported in table 3. The fractional atomic coordinates with thermal parameters, as well as the interatomic bond distances and angles for alacranite are reported in table 4 and 5, respectively, and the corresponding values for realgar are reported in table 6 and 7, respectively. The structural details for alacranite and realgar, corresponding to 72 and 504 hours of thermal treatment, respectively, are best obtained at these stages because such phases are more abundant and well crystallized. Results of Rietveld refinements of the patterns AR72 and AL504 are shown in figures 7 and 8 respectively.

DISCUSSION

This experimental procedure was planned with the aim of examining the different behaviour of the light-induced alteration of natural realgar with the presence of ambient air, or its absence, plus the possible reversibility of the two processes induced by thermal treatments as in the previous work, where the behaviour of β-As_4S_4 have been studied (Zoppi and Pratesi 2012). There are three differences with respect to that conduct experiment: the different starting polymorph – realgar instead of β-As_4S_4 – the additional use of the unfiltered sunlight, which includes also the ultraviolet component, and much longer times of exposure to the heat.

AR series – the presence of the air

The light-induced alteration of realgar, similarly to β-As_4S_4, yields pararealgar, arsenolite and an amorphous phase, but the occurrence of uzonite have never been observed before. Adding the action of the ultraviolet component of sunlight the alteration occurs probably in a sharp and faster way, allowing the formation of As_4S_5 molecules that crystallize in the phase uzonite according to the reaction

proposed by Bindi et al. (2003). When comparing the amount of phases produced in the alteration of realgar to those occurring in the alteration of β-As_4S_4, it is evident that the quantity of amorphous material is much higher in the first case than in the second, 34.39% vs 14.82%, respectively, as well as for the arsenolite formed, 12.58% vs 10.00%, respectively. Correspondingly, the amount or pararealgar is fewer in the first case than in the second, 51.19% vs 75.18%, respectively. As highlighted by Bonazzi et al. (2006) the alteration of realgar into pararealgar requires a complete rearrangement of the molecular packing that passes trough the so called χ-phase, the same packing pattern displayed by β-As_4S_4 and pararealgar. In this view the alteration of realgar means both a bond breaking action and a dislocation of the As_4S_4 molecules, while the alteration of β-As_4S_4 does not require an entire rearrangement of the molecular packing. As pointed out in Zoppi and Pratesi (2012) the mixture of the amorphous phase and pararealgar retains the right As:S ratio to let alacranite crystallize during the thermal treatments, and it is also known that As_xS_y chalcogenide glass materials might display a wide compositional range (Wágner et al. 2003; Krbal et al. 2007; Kaban et al. 2011; González-Leal 2014). As discussed by the authors the presence of both the amorphous phase and arsenolite, plus the unit cell expansion of realgar and β-As_4S_4, cannot be only explained by the reaction $5As_4S_4 + 3O_2 \rightarrow 4As_4S_5 + 2As_2O_3$ (Bindi et al. 2003; Kyono et al. 2005). Nonetheless this reaction must occur, when oxygen is available, since uzonite and arsenolite were detected. According to the QPA results a possible reaction formula, for the light-induced alteration at the stage AR, can be summarized as:

$$7As_4S_4(r) + 3O_2 + h\nu \rightarrow (4\text{-}x/2)As_4S_4(p) + (4\text{-}x)As_2S_3 + xAs_4S_5 + 2As_2O_3$$

where $0<x<1$, though x assumes a small value in this case (~0.1). Differently, according to the reaction formula given for the alteration of β-As_4S_4:

$$9As_4S_4(\beta) + 3O_2 + h\nu \rightarrow 7As_4S_4(p) + 4AsS_2 + 2As_2O_3$$

the light-induced alteration of realgar requires a higher amount of oxygen, for realgar mass, and yields a higher quantity of amorphous phase. Overall we can observe that the molecule As_4S_5 is formed in much higher amount by means of heat than by means of light, as it is shown by the results of QPA. Under the action of the heat the *p*-type molecule formed by the action of the light turns within little time into the *r*-type, since there is no more evidence of pararealgar after one hour of annealing. Differently from the previous experiment (Zoppi and Pratesi 2012), β-As_4S_4 and realgar occur as the heat-induced transformation advances, while alacranite tends to diminish. Arsenolite is approximately constant but occurs in higher amount if compared to the alteration of β-As_4S_4 with the presence of the air. Little amorphous phase is still present after the first step of annealing (AR1), differently from the analogous experiment involving the β-As_4S_4 where there was not any evidence of it. The evolution of the products of alteration of realgar let us suppose that pararealgar and the amorphous phase turn into alacranite, and the latter reacts with the remaining amorphous to yield β-As_4S_4 and realgar, as the annealing process advances. It is not possible to say whether or not the crystallization of β-As_4S_4 and realgar stops for longer time of annealing. At a high degree of heat-induced transformation the Rietveld-RIR method might sometimes yield biased results due to the presence of well developed crystals. Their formation also causes a reduction of the volume of the powder in the capillary and lets empty spaces. Problems in the refinement process might arise by irregular sample displacement, absorption, and crystal orientation effects that are not properly modelled by the software. Fractional coefficients would be required for writing stoichiometric reaction formula of the heat-induced transformation from the stage AR1 to AR504, since the decreasing amount of alacranite and increasing amount of As_4S_4 polymorphs requires the presence of an amorphous phase with increasing sulphur content as the reaction advances:

$$a\mathrm{As_4S_4(p)} + b\mathrm{As_2S_3} + c\mathrm{As_4S_5} + d\mathrm{As_2O_3} \rightarrow e\mathrm{As_8S_9} + f\mathrm{As_4S_4(\beta)} + g\mathrm{As_4S_4(r)} + c\mathrm{As_2O_3} + h\mathrm{As}_x\mathrm{S}_y \quad (x < y)$$

where p, β and r stands for pararealgar, β-As_4S_4 and realgar, respectively, and *a*, *b*, *c*, *d*, *e*, *f*, *g*, and *h* are variable stoichiometric coefficients whose values are determined by the advancement of the reaction. The structure of alacranite formed in the process involving natural realgar (tab. 4 and 5) matches to that described by Zoppi and Pratesi (2012) and exhibits little differences if compared to the natural alacranite described by Bonazzi et al. (2003b), the unit-cell volume measuring 843.53 $Å^3$ vs 857.1 $Å^3$, respectively. Some of the interatomic bond distances for the As_4S_4 molecule are slightly shorter (As1-S1) and some slightly longer (As1-S3*, As2-S3, As1-As2), as it occurs also for the As_4S_5 molecule, with some interatomic bond distances slightly shorter (As3-S6†, As4-S6) and one slightly longer (As4-As4†) than those reported by Bonazzi et al. (2003b). Only one interatomic bond angle in the As_4S_4 molecule (As1-S1-As1*) and one in the As_4S_5 molecule (S6-As4-S4†) exhibit slightly higher values. Non stoichiometric types of alacranite show some structural variations (Bonazzi et al. 2003a; 2006) which are ascribed to a local disordered distribution of the As_4S_4 and As_4S_5 molecules. In this case, given the similar topology of the two molecules, the refined atomic coordinates would represent average values of the positions occupied by analogous atoms belonging to the As_4S_4 and As_4S_5 molecules. This phenomenon also accounts for the slightly high or low isotropic thermal parameters shown by some atoms of the alacranite, as in the case of the U_{iso} of the S2 atom, where it was fixed to an average value (see experimental). These results show that this phase is analogous to the corresponding alacranite formed in the process involving synthetic β-As_4S_4, and let us to hypothesizing that starting either from β-As_4S_4 or realgar the mechanisms driving the reorganization of the altered material is the same. It must be stressed that the alteration of realgar into pararealgar, and the formation of the amorphous phase, occurred under not exactly the same conditions in terms of light, compared to the previous experience (Zoppi and Pratesi 2012). Furthermore a direct comparison with the non-

stoichiometric alacranite obtained by Ballirano (2012), from the thermal treatment of realgar, is not possible since those experiments were carried out on a non-hermetically sealed capillary.

AL series – the absence of the air

The alteration of realgar carried out under isopropyl alcohol had the purpose of preventing the contact with the oxygen. The complete transformation of realgar into pararealgar substantiated that the light-induced alteration is a phenomenon that transforms the *r*-type molecule to the *p*-type without any occurrence of detectable arsenolite, uzonite, and amorphous phase. In the following thermal treatments pararealgar transforms completely into the χ-phase, the expanded form of β-As_4S_4, then β-As_4S_4, and from the stage of 72 hours (AL72), the latter turns into realgar, eventually little orpiment and an amorphous phase forms. This sequence shows that the amount of realgar tends to improve as the heat-induced transformation advances, and exhibits much higher values of weight percent in the AL series than the AR series, for corresponding times. The crystal structure of the synthetic realgar formed after the heat-induced transformation matches well with those reported by the literature. The bond distances As1-S1 and As2-S3 show values about 2% longer and shorter, respectively, than the values given by the authors (Mullen and Nowacki 1972; Kyono et al. 2005), probably due to the fact that the structural refinement from XRPD data of a multiphase powder yields less accurate values if compared to the single crystal technique. These results show that the light-induced alteration of realgar is not completely reversible. In fact the transformation of the β-As_4S_4 into realgar is accompanied by the occurrence of orpiment and an increasing amorphous phase, which means that in some As_4S_4 molecules the As-As and As-S bonds are broken and As_xS_y clusters released. Given the formation of orpiment, and for the closed system to maintain the initial stoichiometry, the amorphous phase must necessarily hold an As:S atomic ratio higher than one, and its chemical formula might be As_xS_y , with *x*

> y. The possible occurrence of such a phase is based on the acknowledgment that molecules such as As_4S_3, As_4S_2 , or As_4S, can exist, as described by Kyono (2013) who investigated their possible structural characteristics using ab initio quantum chemical calculations. Indeed SEM observations show the presence of micrometric-sized material with heterogeneous chemical composition that let us suppose the occurrence of a mixture of chalcogenide glasses of variable chemical formula. In this case the transformation could be schematized as:

$$a As_4S_4(p) \rightarrow b As_4S_4(\beta) + c As_4S_4(r) + d As_2S_3 + e As_xS_y$$

where $x > y$.

For both cases, at longer times of exposure to the heat, the occurrence of orpiment and amorphous phase in the AL series, and the diminishing of alacranite with the presence of amorphous material in the AR series, shows that these are complex phenomena involving multiphase equilibria, the detailed study of which is not the purpose of this work. It must be noticed though, that the heat-induced inverse transformation from pararealgar to realgar takes place through the formation of β-As_4S_4, and that this phase occurs in the stability fields of realgar in both the closed systems, either with alacranite, arsenolite and amorphous material, in the AR series, or with orpiment and amorphous material, in the AL series. This evidence suggests that the combination of all these phases in natural environments should not be ruled out, as the paragenetic association of realgar, orpiment and wakabayashilite, along with bonazziite proves (Bindi et al. 2014).

IMPLICATIONS

When realgar undergoes the alteration induced by light, as it happens for the β-As_4S_4, it exhibits a dual behaviour whether the process occurs with the presence of the air or without it. Different behaviour occurs also when the products are then isolated from the oxygen, and annealed in the realgar stability

field at 220 °C. These evidences show that the transformation of realgar to pararealgar, thus from the *r*-type molecules to the *p*-type ones, is a phenomenon that might occur completely even without the occurrence of other phases, whose growth is triggered by the action of the oxygen, such as arsenolite and uzonite. While the light-induced alteration of β-As_4S_4, occurring without the presence of the oxygen, is completely reversible through the heat, this does not happen with realgar. Once realgar has been completely altered by the action of the light it is possible only to obtain partially the starting material. These evidences point out that in the case of realgar the light causes a broader breaking of As-S and As-As bonds in the lattice, if compared to the β-As_4S_4 alteration, as the higher occurrence of amorphous material shows. Even though realgar transformed completely to pararealgar when altered in isopropyl alcohol we cannot rule out the catalytic action of the oxygen, invoked by Bindi et al. (2003), if that is present in extremely low concentration. This might partially explain the phenomenon of alteration but it is highly unlikely that the same catalytic role might intervene also during the inverse transformation, and does not explain the volume expansion actually observed in the light-induced alteration of As_4S_4 polymorphs. The examination of the inverse transformation of realgar, or the β-As_4S_4, altered by light represents a different approach to the problem of the direct modification of the *r*-type molecule at the base of these polymorphs. This might signify another step into the difficult comprehension of the χ-phase, whose nature has not been thoroughly explained yet.

ACKNOWLEDGEMENTS

We are grateful to Andrea Ienco for the help in XRPD data collection and Daniele Borrini for his help during the thermal treatments. The authors would like to thank Atsushi Kyono and an anonymous reviewer for their valuable comments and suggestions for improving the quality of the paper. This work was founded by the research grant no. 21403(296) of the University of Florence.

REFERENCES CITED

Ballirano, P. (2012) Thermal behavior of realgar As_4S_4, and of arsenolite As_2O_3 and non-stoichiometric As_8S_{8+x} crystals produced from As_4S_4 melt recrystallization. American Mineralogist, 97, 1320–1329.

Ballirano, P., and Maras, A. (2006) In-situ X-ray transmission powder diffraction study of the kinetics of the light-induced alteration of realgar (α-As_4S_4). European Journal of Mineralogy, 18, 589-599.

Bindi, L., Popova, V., and Bonazzi, P. (2003) Uzonite, As_4S_5, from the type locality: single-crystal X-ray study and effects of exposure to light. Canadian Mineralogist, 41, 1463-1468.

Bindi, L., and Bonazzi, P. (2007) Light-induced alteration of arsenic sulfieds: a new product with an orthorhombic crystal structure. American Mineralogist, 92, 617-620.

Bindi, L., Pratesi, G., Muniz- Miranda, M., Zoppi, M., Chelazzi, L., Lepore, G.O., and Menchetti, S. (2014) From ancient pigments to modern optoelectronic applications of arsenic sulfides: Bonazziite, the natural analogue of β-As_4S_4 from Khaidarkan deposit, Kyrgyzstan. Mineralogical Magazine 78, in press.

Bonazzi, P., and Bindi, L. (2008) A crystallographic review of arsenic sulfides: effects of chemical variations and changes induced by exposure to light. Zeitschrift für Kristallographie, 223, 132-147.

Bonazzi, P., Menchetti, S., and Pratesi, G. (1995) The crystal structure of pararealgar, As_4S_4. American Mineralogist, 80, 400-403.

Bonazzi, P., Menchetti, S., Pratesi, G., Muniz-Miranda, M., and Sbrana, G. (1996) Light-induced variations in realgar and β-As_4S_4: X-ray diffraction and Raman studies. American Mineralogist, 81, 874-880.

Bonazzi, P., Bindi, L., Olmi, F., and Menchetti, S. (2003a) How many alacranites do exist? A structural study of non-stoichiometric As_8S_{9-x} crystals. European Journal of Mineralogy, 15, 282-288.

Bonazzi, P., Bindi, L., Popova, V.I., Pratesi, G., and Menchetti, S. (2003b) Alacranite, As_8S_9: structural study of the holotype and re-assignment of the original chemical formula. American Mineralogist, 88, 1796-1800.

Bonazzi, P., Bindi, L., Pratesi, G., and Menchetti, S. (2006) Light-induced changes in molecular arsenic sulfides: State of the art and new evidence by single-crystal X-ray diffraction. American Mineralogist, 91, 1323-1330.

Bonazzi, P., Bindi, L., Muniz Miranda, M., Chelazzi, L., Rodl, T., and Pfitzer, A. (2010) Light-induced molecular change in $HgI_2 \cdot As_4S_4$: evidence by single-crystal X-ray diffraction and Raman Spectroscopy. American Mineralogist, 96, 646-653.

Burgio, L., Clark, R.J.H., and Theodoraki, K. (2003) Raman microscopy of Greek icons: identification of unusual pigments. Spectrochimica Acta, A59, 2371-2389.

Burgio, L., Clark, R.J.H., and Rosser-Owen, M. (2006) Raman analysis of ninth-century Iraqi stuccoes from Samarra. Journal of Archaeological Science, 34, 756-762.

Clark, R.J.H., and Gibbs, P.J. (1997) Identification of lead(II) sulfide and pararealgar on a 13th century manuscript by Raman microscopy. Chemical Communications, 11, 1003-1004.

− (1998) Raman microscopy of a 13th-century illuminated text. Analytical Chemistry News & Features, 70, 99A-104A.

Corbeil, M.-C., and Helwig, K. (1995) An occurrence of pararealgar as an original or altered artists' pigment. Studies in Conservation, 40, 133-138.

Douglass, D.L., Shing, C., and Wang, G. (1992) The light-induced alteration of realgar to pararealgar. American Mineralogist, 77, 1266-1274.

González-Leal, J.M. (2014) Surface and conformational characteristics of $As_{40}S_{60}$ glass films prepared by continuous-wave laser deposition. Materials Research Express 1, 015201.

Gualtieri, A. F. (2000): Accuracy of XRPD QPA using the combined Rietveld-RIR method. Journal of Applied Crystallography, 33, 267-278.

Ito, T., Morimoto, N., and Sadanaga, R. (1952) The crystal structure of realgar. Acta Crystallographica, 5, 775-782.

Kaban, I., Jóvári, P., Wágner, T., Bartoš, M., Frumar, M., Beuneu, B., Hoyer, W., Mattern, N., and Eckert, J. (2011) Structural study of AsS_2–Ag glasses over a wide concentration range. Journal of Non-Crystalline Solids, 357, 3430-3434.

Krbal, M., Wagner, T., Srba, T., Schwarz, J., Orava, J., Kohoutek, T., Zima, V., Benes, L., Kasap, S.O., and Frumar, M. (2007) Properties and structure of $Ag_x(As_{0.33}S_{0.67})_{100-x}$ bulk glasses. Journal of Non-Crystalline Solids, 353, 1232-1237.

Kutoglu, V.A. (1976) Darstellung und Kristallstruktur einer neuen isomeren Form von As_4S_4. Zeitschrift für Anorganische und Allgemeine Chemie, 419, 176-184.

Kyono. A. (2007) Experimental study of the effect of light intensity on arsenic sulfide (As_4S_4) alteration. Journal of Photochemistry and Photobiology A: Chemistry, 189, 15-22.

Kyono. A. (2013) Ab initio quantum chemical investigation of arsenic sulfide molecular diversity from As_4S_6 and As_4. Physics and Chemistry of Minerals, 40, 717-731.

Kyono, A., Kimata, M., and Hatta, T. (2005) Light-induced degradation dynamics in realgar: in situ structural investigation using single-crystal X-ray diffraction study and X-ray photoelectron spectroscopy. American Mineralogist, 90, 1563-1570.

Larson, A.C., and Von Dreele, R.B. (2004) "General Structure Analysis System (GSAS)", Los Alamos National Laboratory Report, LAUR86-748.

Liu, Y., He, P., Liu, F., Zhou, N., Cheng, X., Shi, L., Zhu, H., Zhao, J., Wang, Y., and Zhang, M. (2014) Tetra-arsenic tetra-sulfide (As_4S_4) promotes apoptosis in retinoid acid-resistant human acute promyelocytic leukemic NB4-R1 cells through downregulation of SET protein. Tumor Biology 35, 3421-3430.

Lu, D.P., Qiu, J.Y., Jiang, B., Wang, Q., Liu, K.Y., Liu, Y.R., and Chen, S.S. (2002) Tetra-arsenic tetrasulfide for treatment of acute promyelocytic leukemia: a pilot report. Blood, 99, 3136–3143.

Mullen, D.J.E., and Nowacki, W. (1972) Refinement of the crystal structures of realgar, AsS and orpiment, As_2S_3. Zeitschrift für Kristallographie, 136, 48-65.

Muniz-Miranda, M., Sbrana, G., Bonazzi, P., Menchetti, S., and Pratesi, G. (1996) Spectroscopic investigation and normal mode analysis of As_4S_4 polymorphs. Spectrochimica Acta, A52, 1391-1401.

Naumov, P., Makreski, P., and Jovanovski, G. (2007) Direct atomic scale observation of linkage isomerization of As_4S_4 clusters during the photoinduced transition of realgar to pararealgar. Inorganic Chemistry, 46, 10624-10631.

Porter, E.J. and Sheldrick, G.M. (1972) Crystal structure of a new crystalline modification of tetra-arsenic tetrasulphide (2,4,6,8-tetrathia-1,3,5,7-tetra-arsatricyclo[3,3,0,0]-octane). Journal of the American Chemical Society Dalton, 13, 1347-1349.

Roberts, A.C., Ansell, H.G., and Bonardi, M. (1980) Pararealgar, a new polymorph of AsS, from British Columbia. Canadian Mineralogist, 18, 525-527.

Roland, G.W. (1972) Concerning the α-AsS ↔ realgar inversion. Canadian Mineralogist, 11, 520-525.

Stephens, P.W. (1999) Phenomenological model of anisotropic peak broadening in powder diffraction. Journal of Applied Crystallography, 32, 281-289.

Street, B.G., and Munir, Z.A. (1970) The structure and thermal properties of synthetic realgar (As_4S_4). Journal of Inorganic Nuclear Chemistry, 32, 3769.3774.

Toby, B.H. (2001) EXPGUI, a graphical user interface for GSAS. Journal of Applied Crystallography, 34, 210-213.

Trentelman, K., Stodulski, L., and Pavlosky, M. (1996) Characterisation of pararealgar and other light-induced transformation products from realgar by Raman microspectroscopy. Analytical Chemistry, 68, 1755-1761.

Wágner, T., Krbal, M., Kohoutek, T., Peřina, V., Vlček, Mir., Vlček, Mil., and Frumar, M. (2003) Kinetics of optically- and thermally-induced diffusion and dissolution of silver in spin-coated $As_{33}S_{67}$ amorphous films; their properties and structure. Journal of Non-Crystalline Solids, 326&327, 233-237.

Xiong, X.X., and Liu, C.T. (1998) Mineralogical study of realgar from the Shimen As(Au) deposit, Hunan province. Acta Petrologica et Mineralogica, 378-384.

Zhao, Q.H., Zhang, Y., Liu, Y., Wang, H.L., Shen, Y.Y., Yang, W.J., and Wen, L.P. (2009) Anticancer effect of realgar nanoparticles on mouse melanoma skin cancer *in vivo* via transdermal drug delivery. Medical Oncology, 27, 203-212.

Zoppi, M., and Pratesi, G. (2012) The dual behaviour of the β-As_4S_4 altered by light. American Mineralogist, 97, 890-896.

Zoppi, M., Bindi, L., Rödl, T., Pielnhofer, F., Weihrich, R., Pfitzner, A., and Bonazzi, P. (2013) Light-induced structural changes in $(HgBr_2)_3(As_4S_4)_2$: An X-ray single-crystal diffraction, Raman spectroscopy and *ab initio* study. Solid State Sciences, 23, 88-95.

FIGURE CAPTIONS

Figure 1. XRPD patterns, shown in the range 10-45 $2\theta°$, as collected from the samples of the series AR. The main peaks of pararealgar (p), arsenolite (x), alacranite (a), β-As_4S_4 (β), and yttrium-III oxide (y) are labelled.

Figure 2. XRPD patterns, shown in the range 10-45 $2\theta°$, as collected from the samples of the series AL. The main peaks of pararealgar (p), realgar (r), orpiment (o), and yttrium-III oxide (y) are labelled.

Figure 3. Weight percent of the phases in the samples of the AR series, **a)**, and AL series, **b)**, after each stage of the thermal treatment, as result from the QPA carried out with the Rietveld-RIR method.

Figure 4. Diagram summarizing the results obtained from the light and heat induced transformation of realgar (this work) compared to the results obtained from the corresponding transformations of β-As_4S_4 (Zoppi and Pratesi 2012).

Figure 5. The first segment of the XRPD pattern (10-45° twotheta) of the sample AR, showing three of the most intense peaks of uzonite.

Figure 6. SEM images (secondary electrons) of an orpiment polycrystalline aggregate **a)**, and a realgar crystal **b)**. Raman spectra of the orpiment aggregate **c)** and the realgar crystal **d)**; only the values of the main Raman bands are indicated.

Figure 7. Graphical results (background subtracted) of the refinement of the XRPD pattern of sample AR72. From top to bottom: observed, calculated, residual pattern, and reflections positions for alacranite, arsenolite, β-As_4S_4, and yttrium-III oxide are reported.

Figure 8. Graphical results (background subtracted) of the refinement of the XRPD pattern of sample AL504. From top to bottom: observed, calculated, residual pattern, and reflections positions of realgar, β-As_4S_4, , yttrium-III oxide, and orpiment are reported.

TABLES

Table 1. Weight percent of the phases in the samples of the AR series, after the light-induced alteration and after each stage of the thermal treatment, as result from the QPA carried out with the Rietveld-RIR method.

	AR	AR1	AR72	AR240	AR504
pararealgar	51.2(2)				
arsenolite	12.6(1)	13.1(1)	12.9(1)	12.8(1)	12.1(2)
alacranite		84.4(1)	81.7(1)	65.8(2)	59.9(5)
β-As_4S_4			3.6(1)	16.1(3)	41.9(4)
realgar				2.2(1)	10.8(2)
uzonite	1.8(1)				
amorphous	34.4	2.5	1.8	3.1	-24.7

Table 2. Weight percent of the phases in the samples of the AL series, after the light-induced alteration and after each stage of the thermal treatment, as result from the QPA carried out with the Rietveld-RIR method.

	AL	AL1	AL24	AL72	AL240	AL504	AL672
pararealgar	99.7(1)						
β-As_4S_4		100.1(1)*	97.3(1)*	94.1(1)*	27.9(2)	6.9(2)	4.6(1)
realgar			0.9(1)	4.0(2)	64.9(2)	67.3(1)	63.4(1)
orpiment					3.2(1)	5.2(2)	5.4(2)
amorphous	0.3	-0.1	1.8	1.9	4.0	20.6	26.6
note: * χ-phase							

Table 3. Agreement indices of the refinements, as defined in GSAS (Larson and Von Dreele, 2004) and unit cell parameters for alacranite (sample AR72) and realgar (sample AL504).

AR72	alacranite
R_{wp} = 5.82 % ; R_p = 4.54 %	a = 9.9443(5) Å
χ^2 = 2.52	b = 9.5348(6) Å
$R(F^2)$ = 5.13 %	c = 9.1073(4) Å
arsenolite: $R(F)$ = 3.06 %	β = 102.356(3)°
β-As_4S_4: $R(F)$ = 4.27 %	Vol = 843.53(6) Å^3
standard (Y_2O_3): $R(F)$ = 3.36 %	$R(F)$ = 2.59 %
AL504	realgar
R_{wp} = 5.48 %; R_p = 4.21 %	a = 9.3289(1) Å
χ^2 = 1.79	b = 13.5653(2) Å
$R(F^2)$ = 4.90 %	c = 6.5908(1) Å
β-As_4S_4: $R(F)$ = 2.42 %	β = 106.507(1)°
orpiment: $R(F)$ = 2.94 %	Vol = 799.69(2) Å^3
standard (Y_2O_3): $R(F)$ = 2.14 %	$R(F)$ = 2.83 %

Table 4. Fractional atomic coordinates and isotropic thermal parameters for alacranite (sample AR72).

	x/*a*	*y*/*b*	*z*/*c*	U*iso*
As1	0.0154(6)	0.2111(7)	0.9454(6)	0.028(2)
As2	0.1660(5)	0.4198(7)	0.8695(7)	0.026(2)
As3	0.4546(7)	0.3113(9)	0.4395(8)	0.091(4)
As4	0.3700(6)	0.0364(6)	0.1784(7)	0.029(2)
S1	0	0.088(2)	3/4	0.019(6)
S2	0	0.569(2)	3/4	0.027*
S3	0.195(1)	0.318(1)	0.648(1)	0.023(4)
S4	0.282(1)	0.174(1)	0.334(1)	0.013(4)
S5	1/2	0.446(2)	1/4	0.053(8)
S6	0.385(1)	0.166(1)	-0.005(1)	0.025(4)

* fixed value (see experimental section).

Table 5. Interatomic bond distances (Å) and angles (°) for alacranite (sample AR72).

As_4S_4 molecule		As_4S_5 molecule	
Intramolecular bond distances			
As1-S1	2.113(13)	As3-S6†	2.101(13)
As1-S3*	2.321(12)	As3-S5	2.271(14)
As1-As2	2.669(8)	As3-S4	2.212(12)
As2-S2	2.271(16)	As4-S6	2.111(14)
As2-S3	2.314(14)	As4-S4	2.241(13)
As2-As1	2.669(8)	As4-As4†	2.635(11)
Intramolecular bond angles			
S1-As1-S3*	92.2(5)	S4-As3-S5	105.4(5)
S1-As1-As2	98.1(4)	S4-As3-S6†	102.0(5)
S3-As1-As2	95.3(4)	S5-As3-S6†	109.0(6)
S3-As2-S2	93.4(4)	As4-As4-S6	99.5(5)
S3-As2-As1	95.4(4)	S4-As4-As4†	99.4(4)
S2-As2-As1	101.5(4)	S6-As4-S4†	105.1(5)
As1-S1-As1*	112.2(11)	As3-S4-As4	104.4(5)
As2-S2-As2*	102.6(9)	As3-S5-As3†	111.3(11)
As2-S3-As1*	103.4(5)	As4-S6-As3†	109.7(6)

Notes. symmetry codes: * = -*x*, *y*, 3/2-*z*; † = 1-*x*, *y*, 1/2-*z*.

Table 6. Fractional atomic coordinates and isotropic thermal parameters for realgar (sample AL504).

	x/*a*	*y*/*b*	*z*/*c*	U*iso*
As1	0.1211(3)	0.0208(2)	0.7649(5)	0.045(1)
As2	0.4232(3)	0.8610(2)	0.8532(5)	0.049(1)
As3	0.3223(3)	0.8738(2)	0.1764(4)	0.045(1)
As4	0.0380(3)	0.8385(2)	0.7135(5)	0.049(1)
S1	0.3451(7)	0.0055(5)	0.690(1)	0.054(2)
S2	0.2159(7)	0.0207(5)	0.113(1)	0.049(2)
S3	0.2409(7)	0.7755(5)	0.639(1)	0.048(2)
S4	0.1081(7)	0.7898(5)	0.052(1)	0.051(2)

Table 7. Interatomic bond distances (Å) and angles (°) for realgar (sample AL504).

Intramolecular bond distances			
As1-S1	2.289(7)	As2-As3	2.567(4)
As1-S2	2.212(7)	As3-S2	2.213(7)
As1-As4	2.585(4)	As3-S4	2.243(7)
As2-S1	2.256(7)	As4-S3	2.256(7)
As2-S3	2.207(7)	As4-S4	2.237(7)
Intramolecular bond angles			
S1-As1-S2	95.9(2)	As2-As3-S4	99.2(2)
As4-As1-S1	98.2(2)	S3-As4-S4	94.6(3)
As4-As1-S2	98.7(2)	As1-As4-S3	98.8(2)
S1-As2-S3	93.8(3)	As1-As4-S4	99.2(2)
As3-As2-S1	101.1(2)	As1-S1-As2	99.6(3)
As3-As2-S3	99.8(2)	As1-S2-As3	102.9(3)
S2-As3-S4	94.8(3)	As2-S3-As4	101.7(3)
As2-As3-S2	98.9(2)	As3-S4-As4	101.1(3)

Figure 1

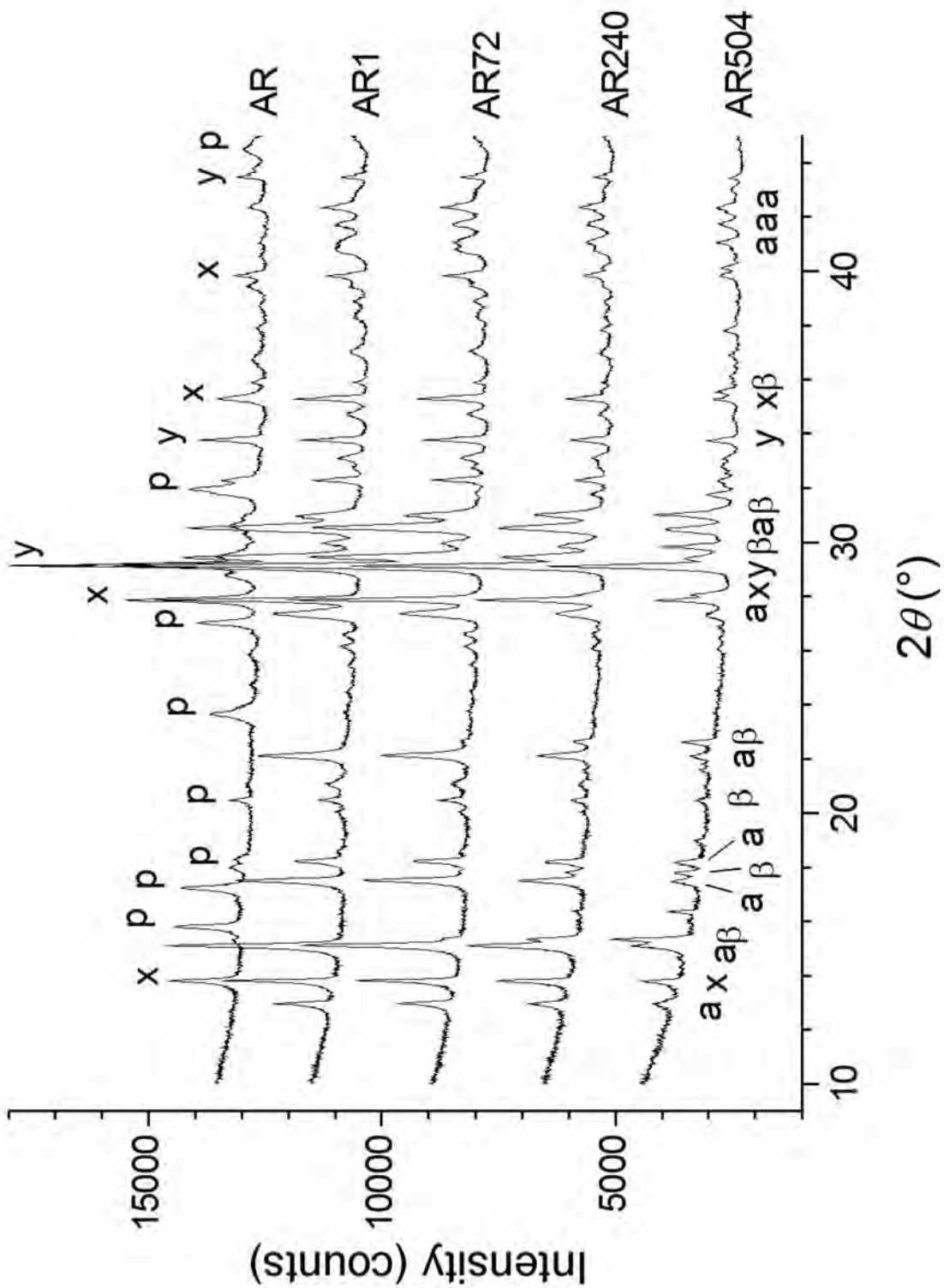
Intensity (counts)
15000
10000
5000
10
20
30
40
2θ(°)
AR
AR1
AR72
AR240
AR504
x p p p p p
y
p y x
x y p
a x aβ
a β a β aβ
axyβaβ
y xβ
aaa

Figure 2

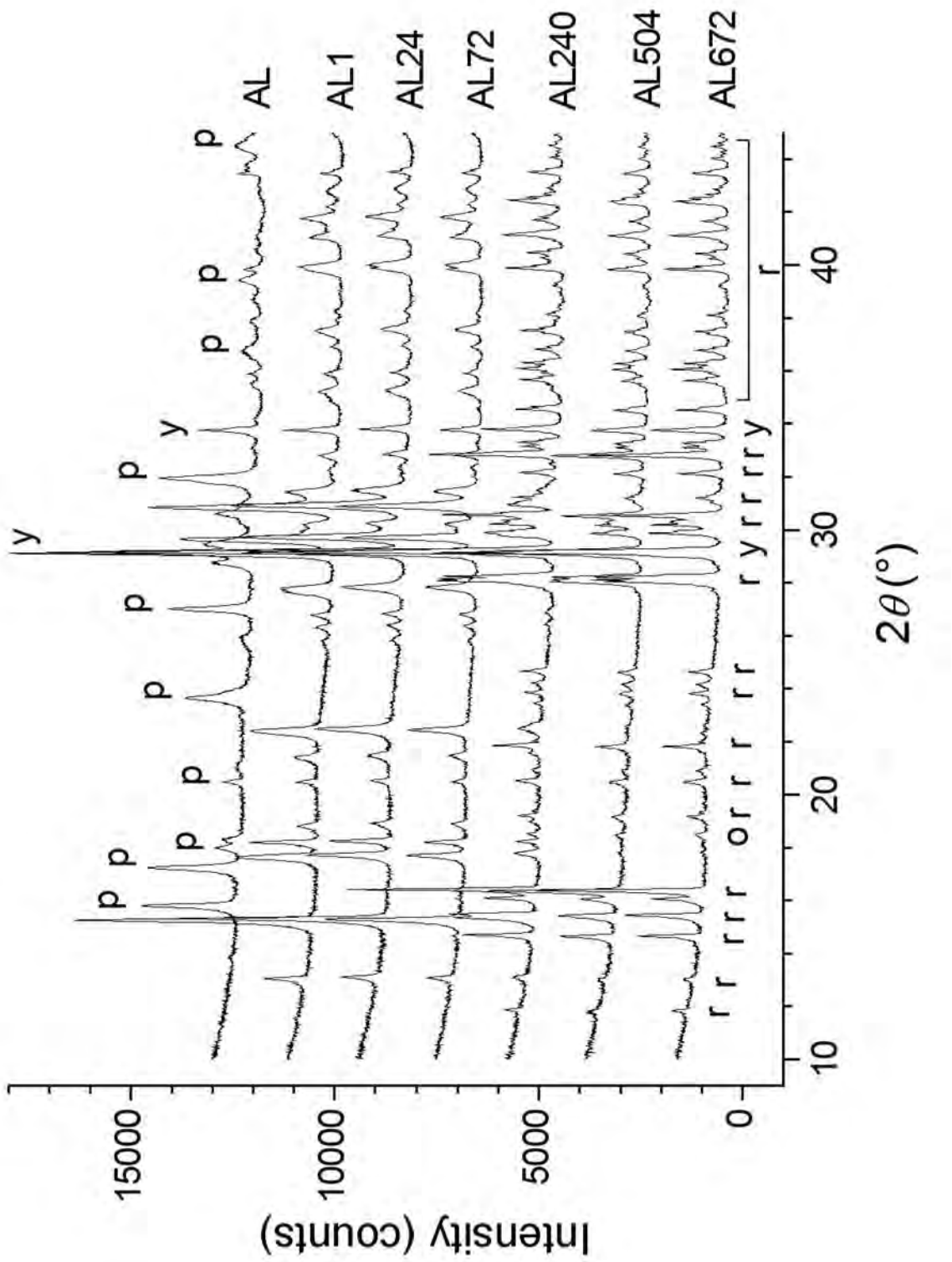
Intensity (counts)
15000
10000
5000
0
10
20
30
40
2θ(°)
AL
AL1
AL24
AL72
AL240
AL504
AL672
p
y
r

Figure 3

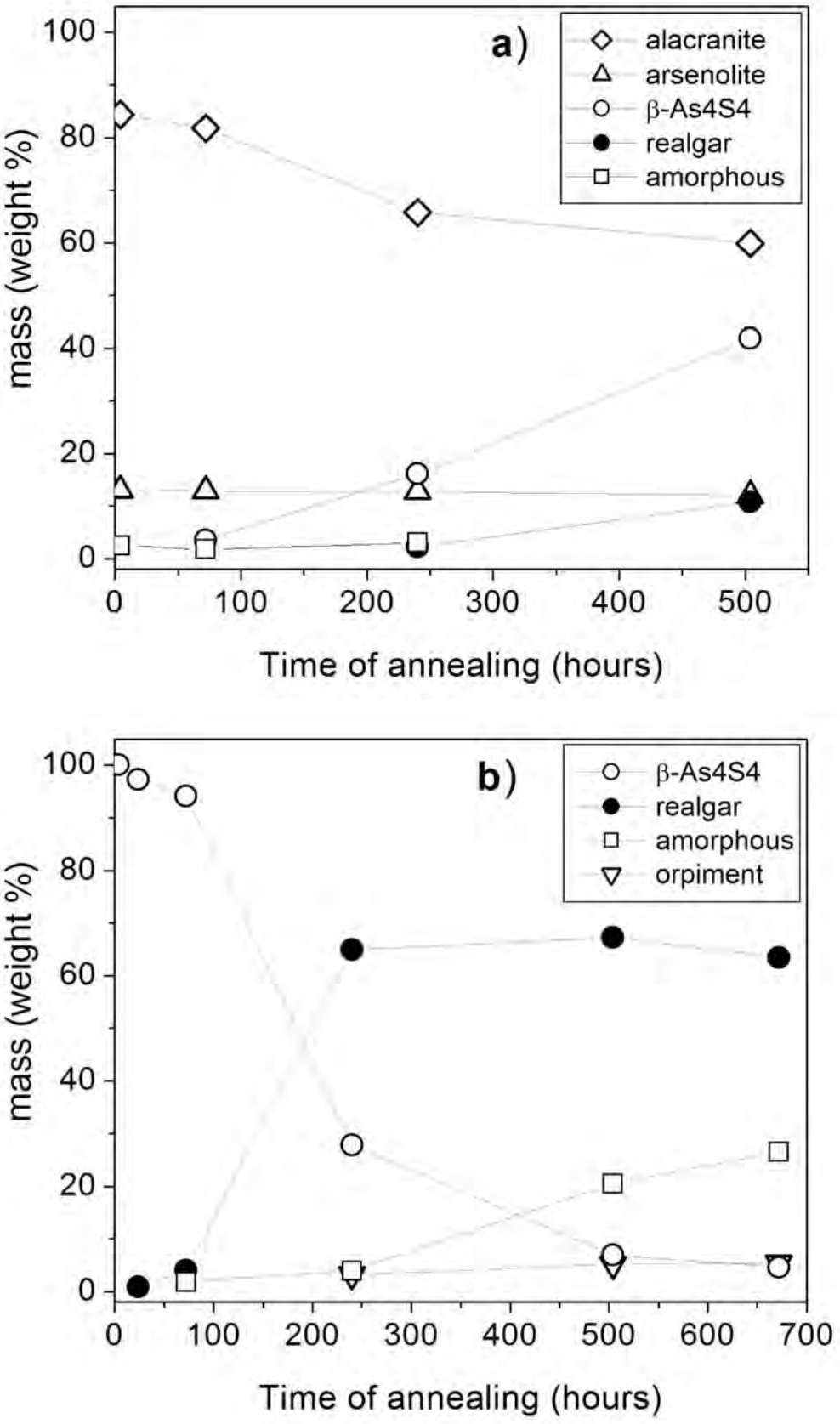
a)
alacranite
arsenolite
β-As4S4
realgar
amorphous
mass (weight %)
Time of annealing (hours)
b)
β-As4S4
realgar
amorphous
orpiment
mass (weight %)
Time of annealing (hours)

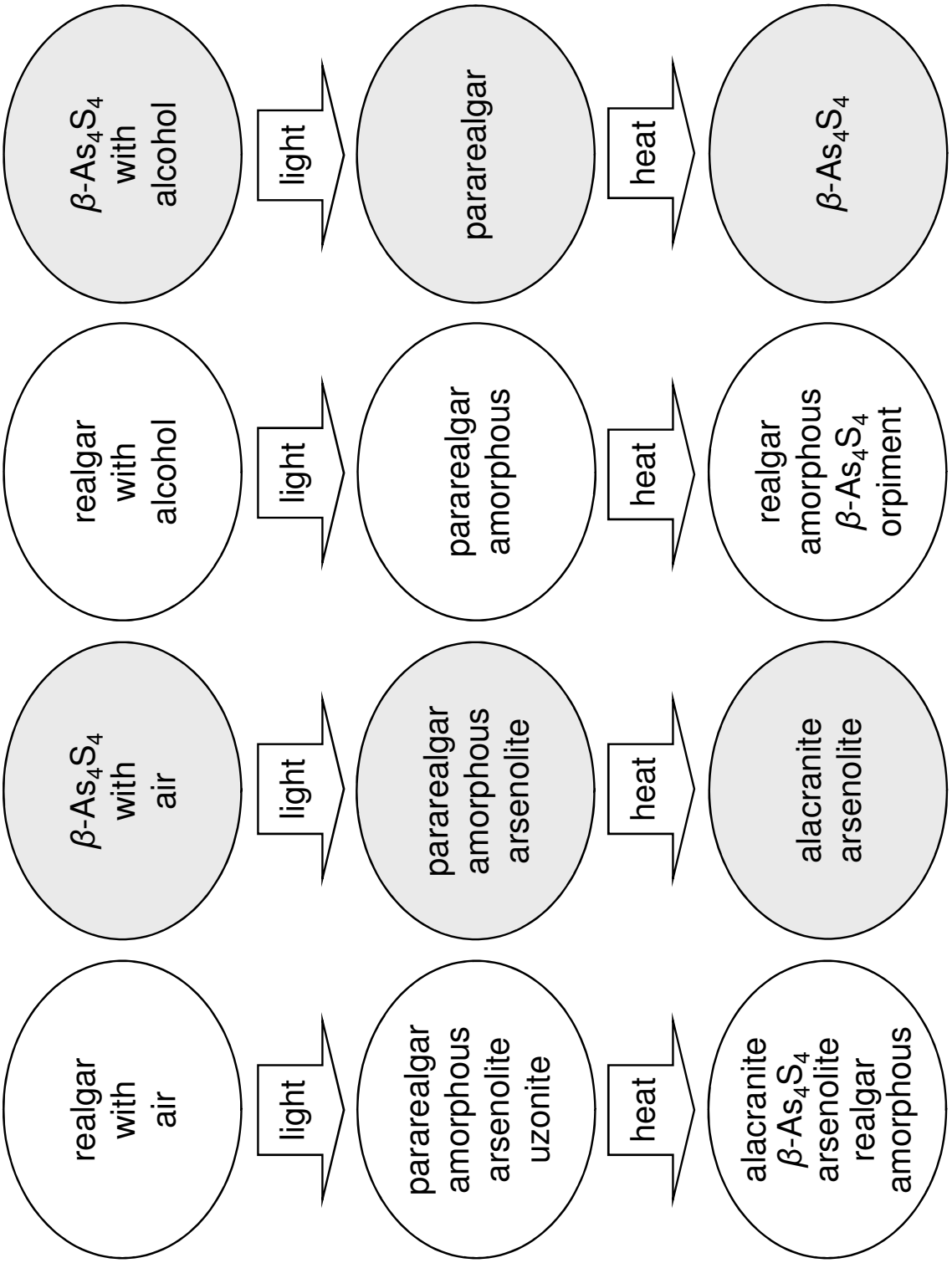
realgar with air
light
parareal gar amorphous arsenolite uzonite
heat
alacranite β-As4S4 arsenolite realgar amorphous
β-As4S4 with air
light
parareal gar amorphous arsenolite
heat
alacranite arsenolite
realgar with alcohol
light
parareal gar amorphous
heat
realgar amorphous β-As4S4 orpiment
β-As4S4 with alcohol
light
parareal gar
heat
β-As4S4

Figure 4

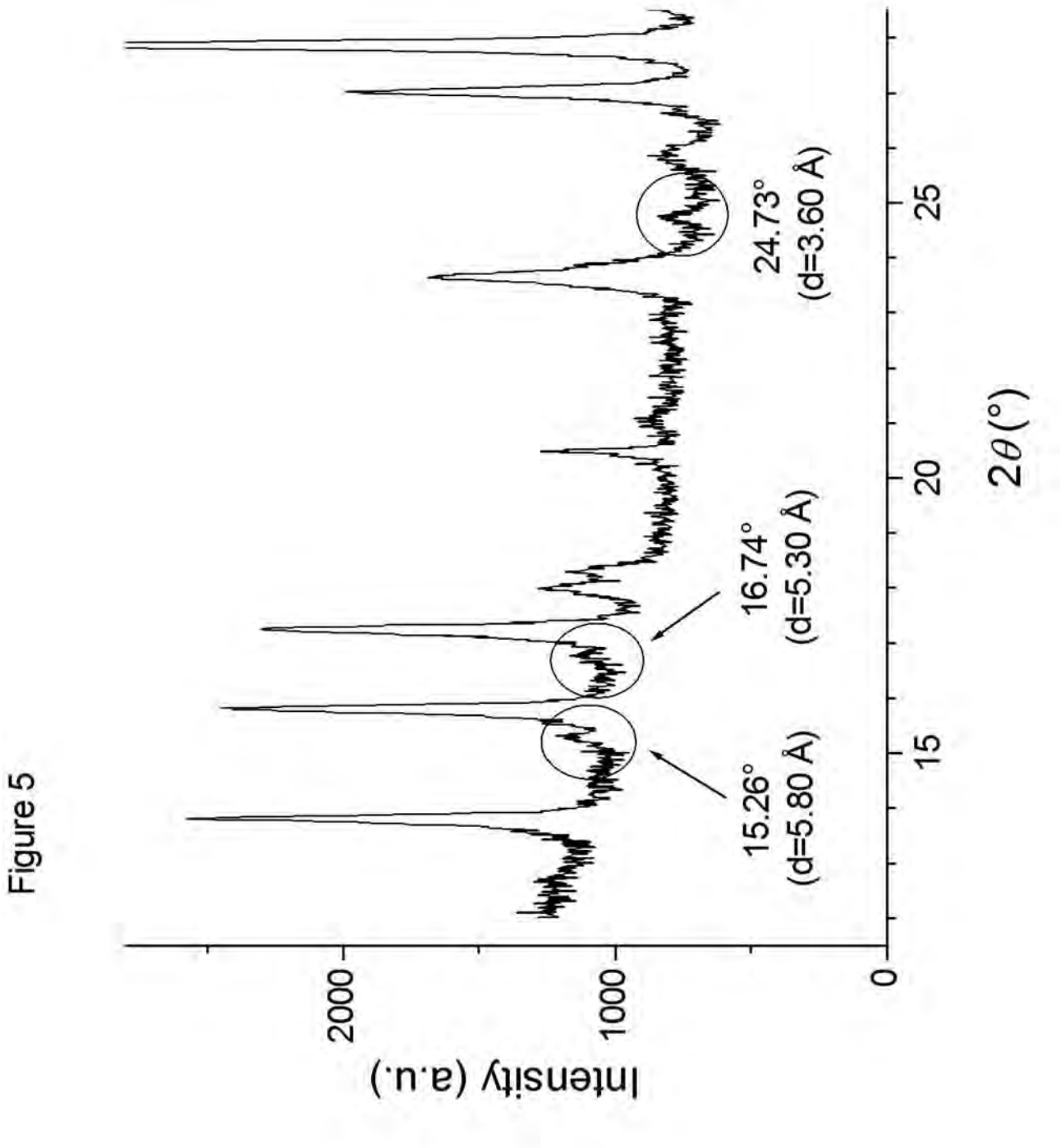
Intensity (a.u.)
2000
1000
0
15
20
25
2θ(°)
15.26°
(d=5.80 Å)
16.74°
(d=5.30 Å)
24.73°
(d=3.60 Å)

Figure 5

Figure 6

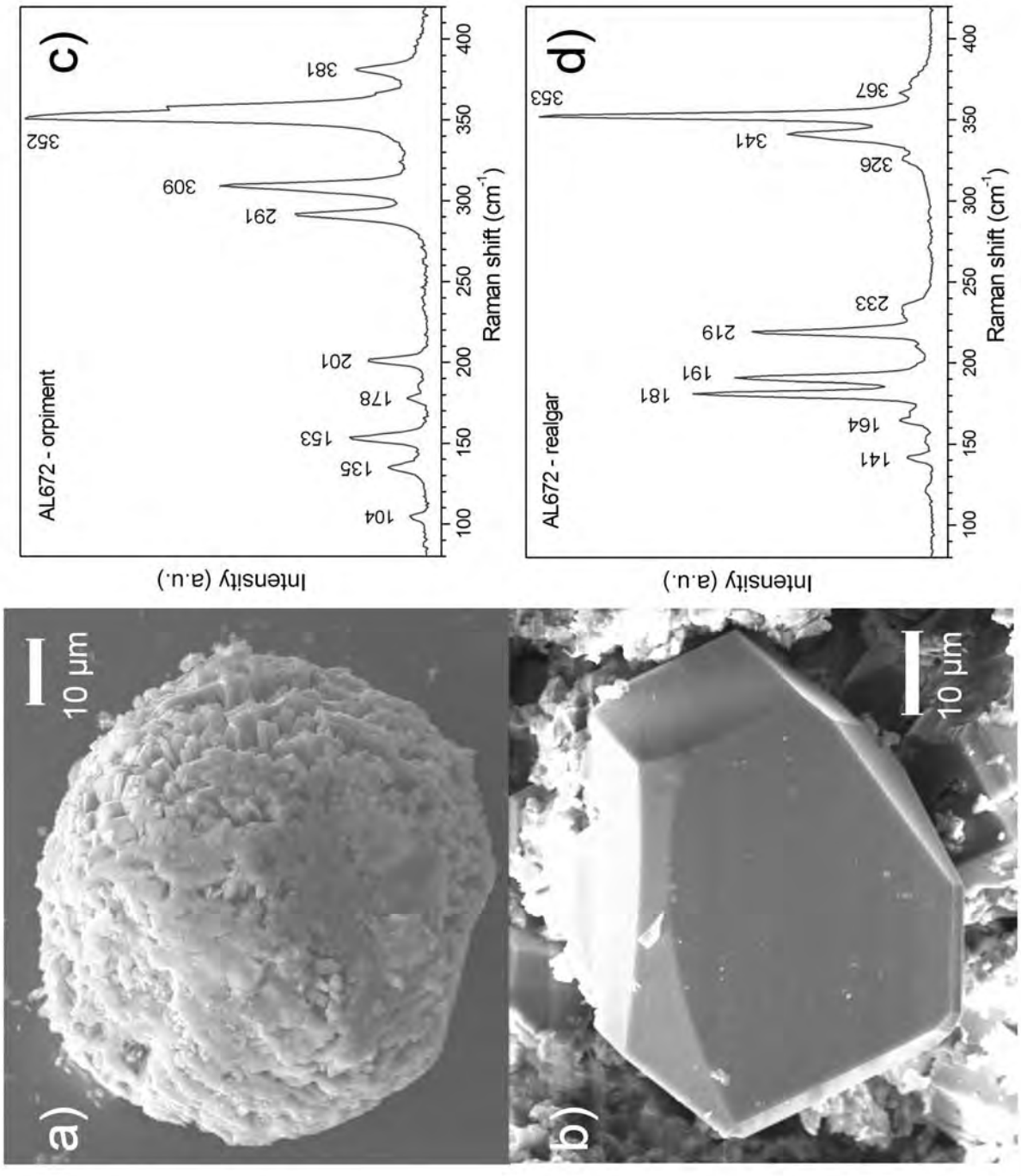
a)
10 µm
b)
10 µm
c)
AL672 - orpiment
104
135
153
178
201
291
309
352
381
Intensity (a.u.)
Raman shift (cm-1)
d)
AL672 - realgar
141
164
181
191
219
233
326
341
353
367
Intensity (a.u.)
Raman shift (cm-1)

Figure 7

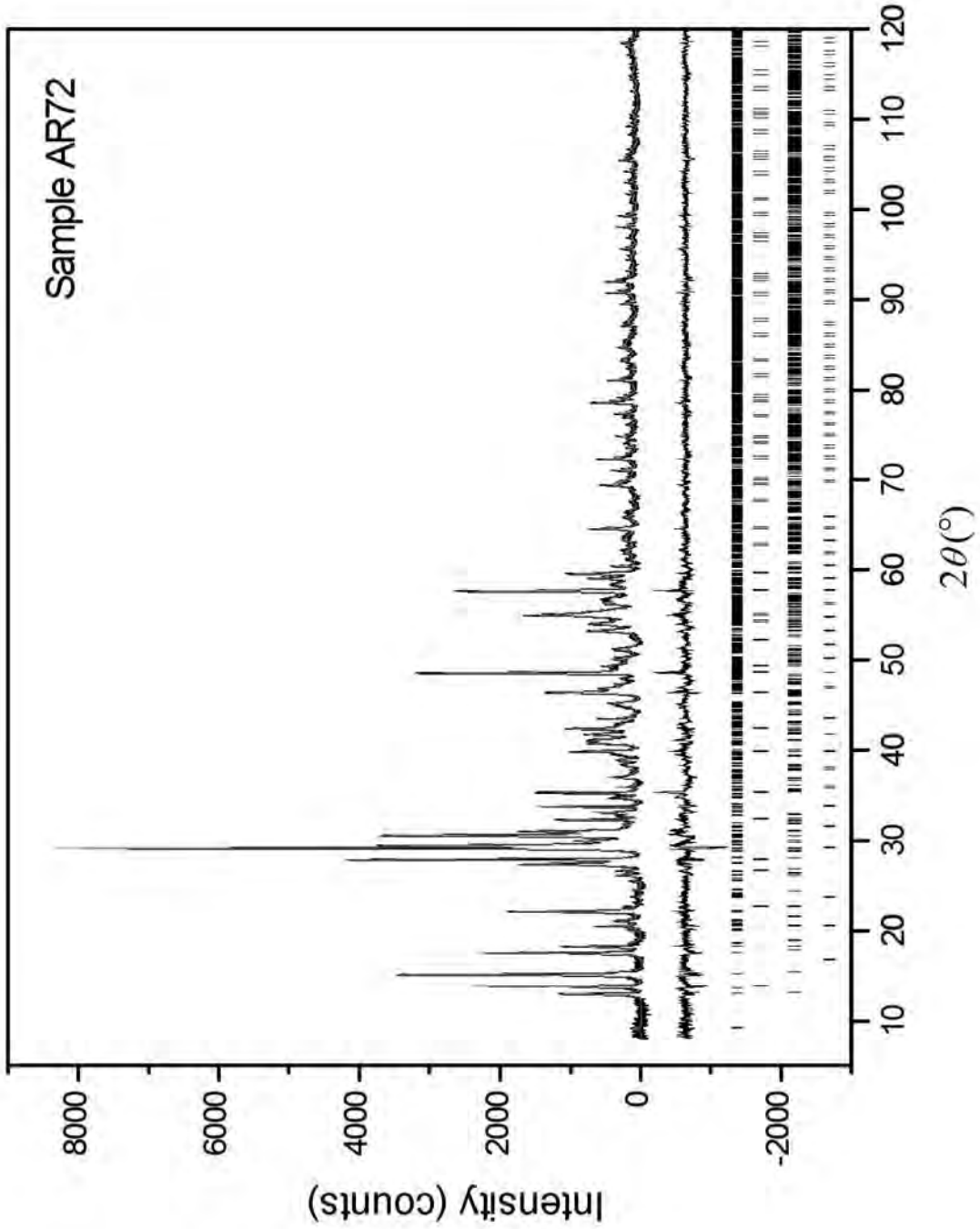
Sample AR72
Intensity (counts)
8000
6000
4000
2000
0
-2000
10
20
30
40
50
60
70
80
90
100
110
120
2θ(°)

Figure 8

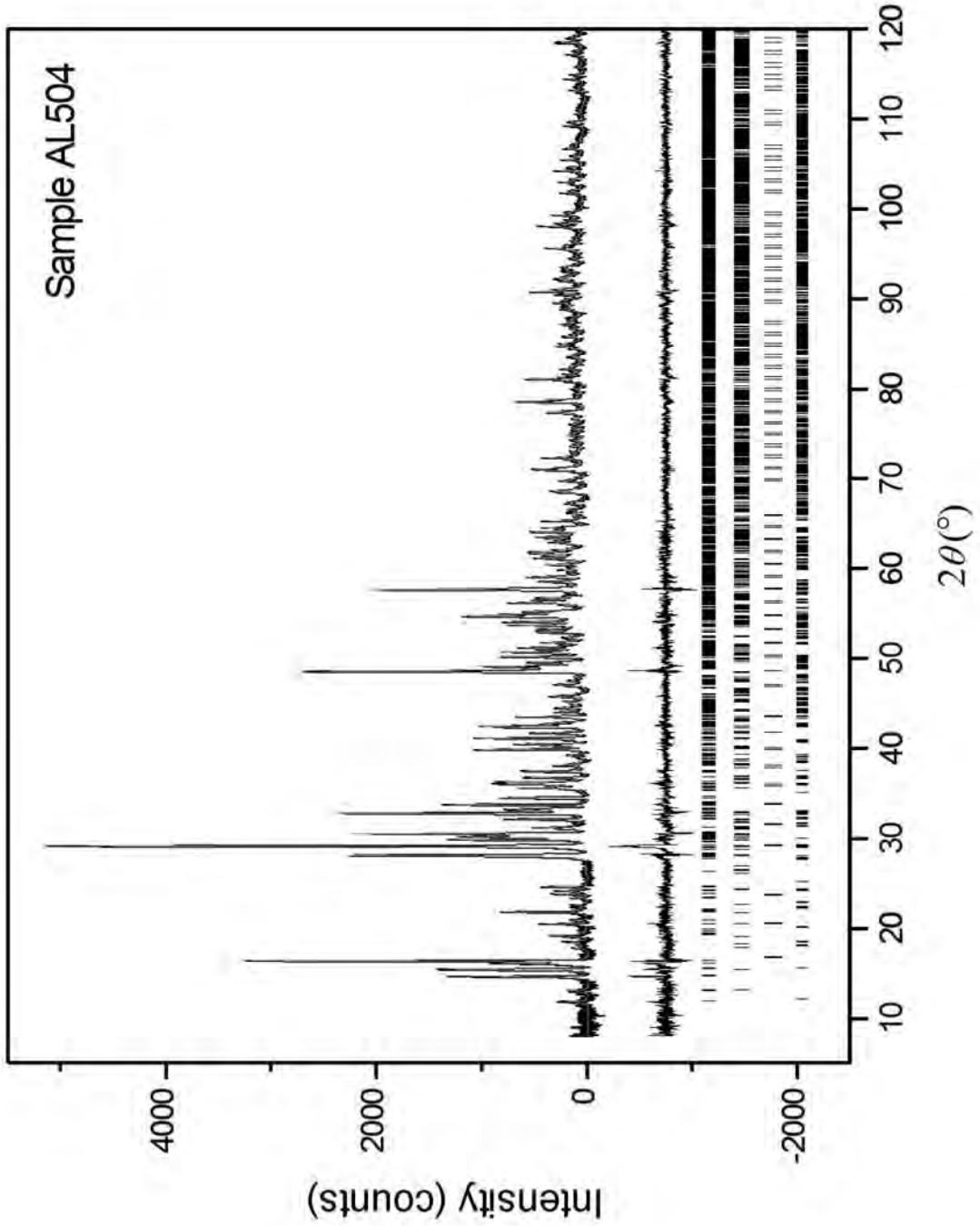
Sample AL504
Intensity (counts)
4000
2000
0
-2000
10
20
30
40
50
60
70
80
90
100
110
120
2θ(°)